Published in final edited form as:

Anal Chem. 2013 December 17; 85(24): 11695–11699. doi:10.1021/ac402169x.

Tunable Membranes for Free-Flow Zone Electrophoresis in PDMS Microchip using Guided Self-Assembly of Silica Microbeads

Yong-Ak Song[1,2,*], **Lidan Wu**[2], **Steven R. Tannenbaum**[2,3], **John S. Wishnok**[2], and **Jongyoon Han**[1,2]

[1]Department of Electrical Engineering and Computer Science, Massachusetts Institute of Technology, 77 Massachusetts Ave., Cambridge, MA 02139

[2]Department of Biological Engineering, Massachusetts Institute of Technology, 77 Massachusetts Ave., Cambridge, MA 02139

[3]Department of Chemistry, Massachusetts Institute of Technology, 77 Massachusetts Ave., Cambridge, MA 02139

Keywords

Microfluidic sample preparation; silica beads; peptide/protein separation; transverse electrophoresis; free-flow zone electrophoresis (FFZE)

INTRODUCTION

To increase the throughput of sample preparation in lab-on-a-chip devices, free-flow zone electrophoresis (FFZE) has widely been adapted to separate the molecules of interest based on the charge-to-mass ratio from a sample volume of ~100 μL in a continuous fashion. Several approaches have already been taken to develop continuous free-flow zone electrophoresis in a microfluidic chip format.[1–3] The key engineering issue has been how to couple an electric field efficiently into the sorting process while creating a hydrodynamic barrier between the separation channel and the electrode reservoirs. So far, acrylamide gels[4,5,6], microchannels[7–17], partitioning[18,19] and dielectric materials such as glass[20] have been used as salt bridges. Curing the acrylamide gel inside the PDMS devices, however, has been challenging due to the oxygen barrier on the surface and, therefore, glass has been used as alternative material despite requirements for complex fabrication and separate masks for the polymerization of the membranes. In addition, gel membranes show limited stability under hydrodynamic pressure-driven flow.[21] Although an open connection between the separation channel and the reservoirs allowed the highest electric field across the separation channel[8], control of the flow rate was challenging, requiring a high flow rate of the electrolytes in the side channels at [10–20] μL/min. Recently, the same group has used channel depth variation to control the flow in a [20] μm deep separation channel versus a 78 μm electrode channel and achieved ~91% coupling efficiency of applied voltage.[9] Using higher channel depth to control buffer flow over the electrodes increased the linear velocity ~15 times that of the buffer in the separation channel and removed electrolysis products for more

CORRESPONDING AUTHOR: Tel. 1-617-253-2290, Fax. 1-617-258-5846, jyhan@mit.edu.

*Currently affiliated with the Division of Engineering, New York University Abu Dhabi (NYUAD), P.O. Box 129188, Abu Dhabi, UAE and the Department of Chemical and Biomolecular Engineering, Polytechnic Institute of New York University, Brooklyn, NY 11201

"Supporting Information Available: This material if available free of charge via the Internet at http://pubs.acs.org"

stable separation process. A dielectric wall is another available solution for the membrane, allowing 50% of the electric field without constant flow of the electrolyte solutions.[20] However, glass chips require wet etching steps and they are therefore more difficult to fabricate than PDMS chips.

In this paper, we are demonstrating a simple fabrication method of high-aspect-ratio membranes for free-flow zone electrophoresis in microfluidic PDMS devices. To meet the requirements of an efficient coupling of the voltage from the electrode channels into the sorting channel while offering sufficient hydrodynamic resistance, we have utilized self-assembled microbeads after plasma bonding to a PDMS chip to create a nanoporous junction between the sorting channel and the electrode channel. A similar approach has been proposed by the Jensen group with PMMA microbeads.[22] However, a tunable membrane hasn't been demonstrated. These pores with approximately 15% of the bead diameter, act as a salt bridge between the sorting channel and electrode channels. Additionally, the pores allow infiltration of hydrogel solutions to modify the surface charge of the microbead membrane on each side independently. This surface charge modification allows building an ion-selective membrane that can minimize a migration of the charged molecules to the opposite-polarity electrode, thus reducing a sample loss through the membrane during free-flow electrophoresis. Molecules, especially those with high or low pI values, are deflected through the membrane at high electric field and are lost into the electrode reservoir. For electrical connection, we continuously filled the electrode channels with a strong electrolyte solution such as 3M KCl, and placed Pt wires directly above each electrode channel outlet.[23] In this way, a voltage could be applied across the sorting channel without the bubble formation by electrolysis affecting the sorting process and without adding a redox-couple to the electrolyte[24]. With this device, we demonstrated free-flow separation of peptides and dyes at flow rates up to 2 μL/min and validated the sample loss after sorting with a UV-Vis spectrophotometer. Compared to other previously published microfluidic free-flow zone electrophoresis devices, our sorting chip with a mechanically robust and chemically tunable membranes allows an electrical coupling efficiency of up to 52% (comparable to the dielectric wall device with 50% coupling efficiency[25], however, lower than the multiple-depth micro free-flow zone electrophoresis device with 91% coupling efficiency[9]) at minimal dilution and sample loss. This can lead to a powerful pI-based peptide / protein separation tool with minimal sample loss in a high-throughput fashion.

MATERIALS AND METHODS

Chip Fabrication, Device Operation and Materials/Reagents

See supporting information.

Microbead Preparation

We used three different sizes of the silica beads for the packing process (3, 4, 5 μm, all from Polysciences Inc.) and 6 μm polystyrene beads (Polysciences Inc.). To increase the flowability of the beads into the microchannel, we sonicated the bead suspension in an ultrasonic bath for 30 min. Prior to sonication, we exchanged the DI solution of the bead suspension with a 1 mM poly(L-lysine)-grafted-poly(ethylene glycol) (or PLL-g-PEG) copolymers. The advantage of exchanging the solution is that the PLL-PEG can be used to passivate the surface of the microchannel against non-specific binding during the evaporation-driven packing process of microbeads and it helps to reduce the electroosmotic flow (EOF). The polycationic PLL backbone interacts with the negatively-charged surface and builds a monolayer.[26] To increase the packing density, the PDMS channel was filled with a bead suspension immediately after oxygen plasma bonding while it was still hydrophilic. Once the bead channel has been filled, it was dried out completely inside the

device for overnight. To modify the surface charge, we used a cation-selective hydrogel solution (40%) to fill the porous structure on the cathodic side of the sorting channel and an anion-selective hydrogel solution (40%) on the anodic side of the channel and cured them completely under UV light for 30 min. To make 40% hydrogel, we prepared HEMA (monomer) with acrylic acid (for negatively-charged hydrogel)/DMEAEMA (for positively-charged hydrogel), EGDMA (cross linker) and DMPA (photoinitiator) at a ratio of 60:24:2:4 wt%.[27] To improve the filling characteristic of the anion-selective hydrogel solution in the porous silica matrix, we reduced the content of DMEAEMA from 40% down to 30%.

Measurement with NanoDrop 2000 Spectrophotometer

To quantify the sorting result and sample loss after each sorting process, we collected 10 μL of the sorted samples at the end of the device with inverted pipette tips and analyzed them with a Spectrophotometer (Thermo Scientific Inc., NanoDrop 2000, NC). For UV measurement, only a micro drop of 1 μL sample was required.

RESULTS AND DISCUSSION

To meet the requirement of an efficient coupling of the electrical field while creating sufficient hydrodynamic resistance of the membrane to the sample flow during free-flow zone electrophoresis, we have used an evaporation-driven microbead self-assembly method.[28, 29] In Figure 1a, the schematic of such a μFFZE (micro free-flow zone electrophoresis) device with a single inlet is shown. To trap the microbeads in the bead filling channels, we used an array of cylindrical pillars patterned with a different gap size (1, 2 or 3 μm) on both sides of the bead packing channel. For secure trapping, the microbeads used were at least 2 μm larger than the gap size. Previously, our microfluidic sorting device had three inlets with two inlets for buffer solutions to focus the sample flow hydrodynamically.[23] This, however, caused an excessive dilution of the sample. To avoid this problem, a single inlet design has been adapted without hydrodynamic focusing. Such a single inlet sorting device in PDMS is shown in Figure 1b along with a microbead membrane inside the device (Figure 1c). The sorting channel was 1 mm wide, 5 mm long and [13] μm deep. The sample mixture was binary sorted into positively and negatively charged samples through two outlet channels. However, this new design required a longer migration length of sample molecules for complete separation, rendering the need for efficient electric field coupling in the device crucial. To validate the sorting capability of the device with a 3 μm bead membrane, we first tested a negatively charged Alexa Fluor 488 dye in 5 mM buffer solution at pH 7.0. The dye was deflected towards the anodic side when $V_{applied}$ = 50 V was applied, as shown in Figure 1d. Using the same electric field, a mixture of two pI markers, pI 5.1 and 8.1, was separated into two streams and binary sorted into two different outlets, as shown in Figure 1e.

To characterize the self-assembled microbead membranes, we measured I–V curves of different bead sizes, as shown in Figure 2. In the case of the 3 μm, 4 μm and 5 μm silica beads, the effectively coupled electric field could be calculated with the measured total current i_{total} at a given voltage, e.g. 50 V. For the 3 μm silica bead membrane, the effective potential across the sorting channel was $V_{effective}=V_{applied}-V_{junction}-V_{electrode}$= 18.22 V when $V_{applied}$ = 50 V was applied (see the calculation of effectively coupled electric field for different bead sizes in supporting information). This result means that ~36% of the applied potential was coupled through the 3 μm silica particle membrane into the sorting process. The coupling efficiency increased to ~44% with the 4μm beads and to ~52% with the 5 μm beads. This coupling efficiency is comparable to that of the glass-walled FFZE device.[25] As these results demonstrated, we can tune the effectively coupled electric field into the sorting process by varying the microbead size and thereby its corresponding pore size.

Being a porous solid matrix, the microbead membranes allow for an infiltration of hydrogel solutions. In this way, the porosity of the microbead membranes can be reduced and the surface charge altered on each side differently. This altered surface charge can be utilized to minimize the loss of a sample through the microbead membrane during free-flow electrophoresis. The polarity of the electrodes has to be selected according to the ion selectivity of the membranes (anode paired with the cation-selective and cathode paired with the anion-selective hydrogel membrane). However, coupling efficiency of the electric field is affected by the infiltration of a hydrogel, as shown in Figure 2b. After infiltration with a hydrogel, the effective coupling efficiency decreased to ~33% for all three microbead sizes.

To characterize the sorting efficiency at different electric field strengths, flow rates and particle sizes, we used two pI markers, pI 5.1 and 8.1, and measured the fluorescence intensity profiles across the sorting channel just before the bifurcation, as shown in Figure 1e. The sorting efficiency η, measured as a ratio of the fluorescence intensity before and after sorting in the middle of the sorting channel (x = 500 μm) where the separated samples were bifurcated, increased with higher electric field strength and reached ~85% at E_{effect} = 52.8 V/cm in the case of 4 μm bead device (see Figure S-1 and Table S-1 in supporting information). By increasing the residence time two-folds (through decreasing the flow rate from ^{2} μL/min to 1 μL/min), sorting efficiency of 85% could be reached at E_{effect} = 39.6 V/cm (see Figure S-2 and Table S-2 in supporting information). With a larger pore size (5 μm), sorting efficiency of 82% could be achieved at E_{effect} = 41.6 V/cm and 95% at E = 72.8 V/cm (see Figure S-3 and Table S-3 in supporting information). A summary of this parameter study is given in Figure S-4. Comparable field strength (50 V/cm) was applied to achieve a stable separation in multiple-depth device at a buffer flow rate of 0.375 mL/min.[3,30] In another PDMS device, fluorescein, rhodamine 110 and labeled amino acids were separated at electrical field strength of 137 V/cm[7], while in glass devices, higher electric fields up to 586 V/cm were possible. To demonstrate the effect of surface charge on minimizing sample losses, we used a negatively charged dye, Alexa Fluor 488, as a test sample. The microbead membranes were infiltrated and sealed with a positively and negatively charged hydrogel. First, the dye was contained in a sorting channel without applying a voltage across, as shown in Figure 3a. When a voltage of E_{effect} = 36 V/cm was applied across the sample flow, the negatively charged dye was deflected towards the anode, but blocked by the cation-selective hydrogel membrane, as shown in Figure 3b. When the polarity of the electrode was reversed, however, the negatively charged dye was passing through the anion-selective membrane into the electrode reservoir towards the anode (Figure 3c). As demonstrated in this example, exploiting the ion selectivity of the hydrogel-infiltrated microbead membranes can lead to a significant decrease in sample loss during free-flow electrophoresis, which has not been demonstrated previously. We used these hydrogel-infiltrated microbead membranes to separate two pI markers, as shown in Figure S-5 (see supporting information). Negatively charged pI marker 5.1 was deflected to the anodic side, but was clearly repelled from the cation-selective membrane. On the cathodic side, positively charged pI marker 8.1 was also retained by the anion-selective membrane.

In addition to the fluorescence microscopy, we also verified the sorting result with a UV-spectrometer. Using pI marker 4.0 in pH 7.0 buffer solution, we quantified the sorting result before and after sorting by collecting the fractionated samples out of the device. Without applying a voltage, both the anodic and cathodic sides showed approximately equal distribution of the pI marker (Figure S-6a in supporting information). After sorting, the anodic side showed an increase of the negatively charged pI marker by ~73%, while there was a removal of the pI marker by ~78% on the cathodic side. The comparison of the total absorbance from the collected samples without (0 V) and with sorting (80 V) showed a difference of only 0.04 (see Table S-4 in supporting information). In the case of a positive peptide with pI 10.3, it was removed by ~95% from the anodic side while it was increased

by ~106% on the cathodic side (Figure S-6b in supporting information). The comparison of the total absorbance before and after sorting showed again that the sample loss through the membrane was also minimal with a difference of only 0.09 (see Table S-5 in supporting information).

CONCLUSIONS

We have developed a free-flow zone electrophoresis device in PDMS with membranes out of self-assembled microbeads. By using different silica microbead sizes for packing inside the microchannel, we were able to control the amount of the electric field coupled into the continuous-flow sorting process from 36% up to 52%. Furthermore, the porous microbead membrane allowed infiltration of hydrogel solutions so that the surface charge of the membrane can be tuned to act as an ion-selective membrane. By infiltrating and sealing with a negatively and positively charged hydrogel in the microbead membranes inside the same device, we could prevent the sample from crossing the ion-selective membranes into the electrode channel when deflected under electric field. With the help of these hydrogel-infiltrated bead membranes, we could separate the pI markers and validated a near loss-free recovery confirmed by the UV spectral analysis. The microbead membranes combine the advantages of tunability in terms of the amount of coupled electric field and the rich surface chemistry available for silica beads with the robustness of the membrane for pressure-driven, high-throughput pI-based fractionation of proteins and peptides. The microbead-based membrane opens up further opportunities to implement temperature-, pH- and ionic strength-controlled gating in a micro-nanofluidic platform and to study nanofluidic transport which offers unique opportunity for chemical operations such as molecular concentration and ion selection of biomimetic membranes. Using this tunable membrane, it would be possible to control the permeability in-situ depending on the size and charge of molecules.

Supplementary Material

Refer to Web version on PubMed Central for supplementary material.

Acknowledgments

This work was supported by NIH R21 EB008177-01A2. We thank the staff of MIT Microsystems Technology Laboratory for the support during fabrication and R. Kwak for preparation of hydrogel solutions.

References

1. Pamme N. Lab Chip. 2007; 7:1644–1659. [PubMed: 18030382]
2. Kohlheyer D, Eijkel JCT, van den Berg A, Schasfoort RBM. Electrophoresis. 2008; 29:977–993. [PubMed: 18232029]
3. Turgeon RT, Bowser MT. Anal Bioanal Chem. 2009; 394:187–198. [PubMed: 19290514]
4. Albrecht J, Jensen K. Electrophoresis. 2006; 27:4960–4969. [PubMed: 17117380]
5. Albrecht J, El-Ali J, Jensen K. Anal Chem. 2007; 79:9364–9371. [PubMed: 17994708]
6. Kohlheyer D, Besselink G, Schlautmann S, Schasfoort RBM. Lab Chip. 2006; 6:374–380. [PubMed: 16511620]
7. Zhang CX, Manz A. Anal Chem. 2003; 75:5759–5766. [PubMed: 14588015]
8. Fonslow B, Bowser M. Anal Chem. 2005; 77:5706–5710. [PubMed: 16131085]
9. Fonslow B, Barocas V, Bowser M. Anal Chem. 2006; 78:5369–5374. [PubMed: 16878871]
10. Kobayashi H, Shimamura K, Akaida T, Sakano K, Tajima N, Funazaki J, Suzuki H, Shinohara E. J Chromatogr A. 2003; 990:169–178. [PubMed: 12685595]
11. Becker M, Marggraf U, Janasek D. J Chromatogr A. 2009; 1216:8265–8269. [PubMed: 19631324]
12. Fonslow BR, Bowser MT. Anal Chem. 2008; 80:3182–3189. [PubMed: 18351751]

13. Raymond DE, Manz A, Widmer HM. Anal Chem. 1994; 66:2858–2865.
14. Xu Y, Zhang CX, Janasek D, Manz A. Lab Chip. 2003; 3:224–227. [PubMed: 15007450]
15. Janasek D, Schilling M, Franzke J, Manz A. Anal Chem. 2006; 78:3815–3819. [PubMed: 16737242]
16. Becker M, Mansouri A, Beilein C, Janasek D. Electrophoresis. 2009; 30:4206–4212. [PubMed: 20013904]
17. Becker M, Budich C, Deckert V, Janasek D. Analyst. 2009; 134:38–40. [PubMed: 19082172]
18. Kohler S, Weilbeer C, Howitz S, Becker H, Beushausen V, Belder D. Lab Chip. 2011; 11:309–314. [PubMed: 21060908]
19. Kohler S, Benz C, Becker H, Beckert E, Beushausen V, Belder D. Rsc Adv. 2012; 2:520–525.
20. Janasek D, Schilling M, Manz A, Franzke J. Lab Chip. 2006; 6:710–713. [PubMed: 16738720]
21. Kohlheyer D, Eijkel JC, Schlautmann S, van den Berg A, Schasfoort BM. Anal Chem. 2007; 79:8190–8198. [PubMed: 17902700]
22. Albrecht, J.; Gaudet, S.; Jensen, KF. 9th International Conference on Miniaturized Systems for Chemistry and Life Sciences; Boston, MA. 2005. p. 1537-1539.
23. Song YA, Chan M, Celio C, Tannenbaum SR, Wishnok JS, Han J. Anal Chem. 2010; 82:2317–2325. [PubMed: 20163146]
24. Kohlheyer D, Eijkel JCT, Schlautmann S, van den Berg A, Schasfoort RBM. Anal Chem. 2008; 80:4111–4118. [PubMed: 18435546]
25. Janasek D, Schilling M, Manz A, Franzke J. Lab Chip. 2006; 6:710–713. [PubMed: 16738720]
26. Ruiz-Taylor LA, Martin TL, Zaugg FG, Witte K, Indermuhle P, Nock S, Wagner P. PNAS. 2001; 98:852–857. [PubMed: 11158560]
27. Kim P, Kim SJ, Han J, Suh KY. Nano Lett. 2010; 10:16–23. [PubMed: 20017532]
28. Zeng Y, Harrison DJ. Anal Chem. 2007; 79:2289–2295. [PubMed: 17302388]
29. Zeng Y, He M, Harrison DJ. Angewandte Chemie. 2008; 47:6388–91. [PubMed: 18624306]
30. Turgeon RT, Bowser MT. Electrophoresis. 2009; 30:1342–1348. [PubMed: 19319908]

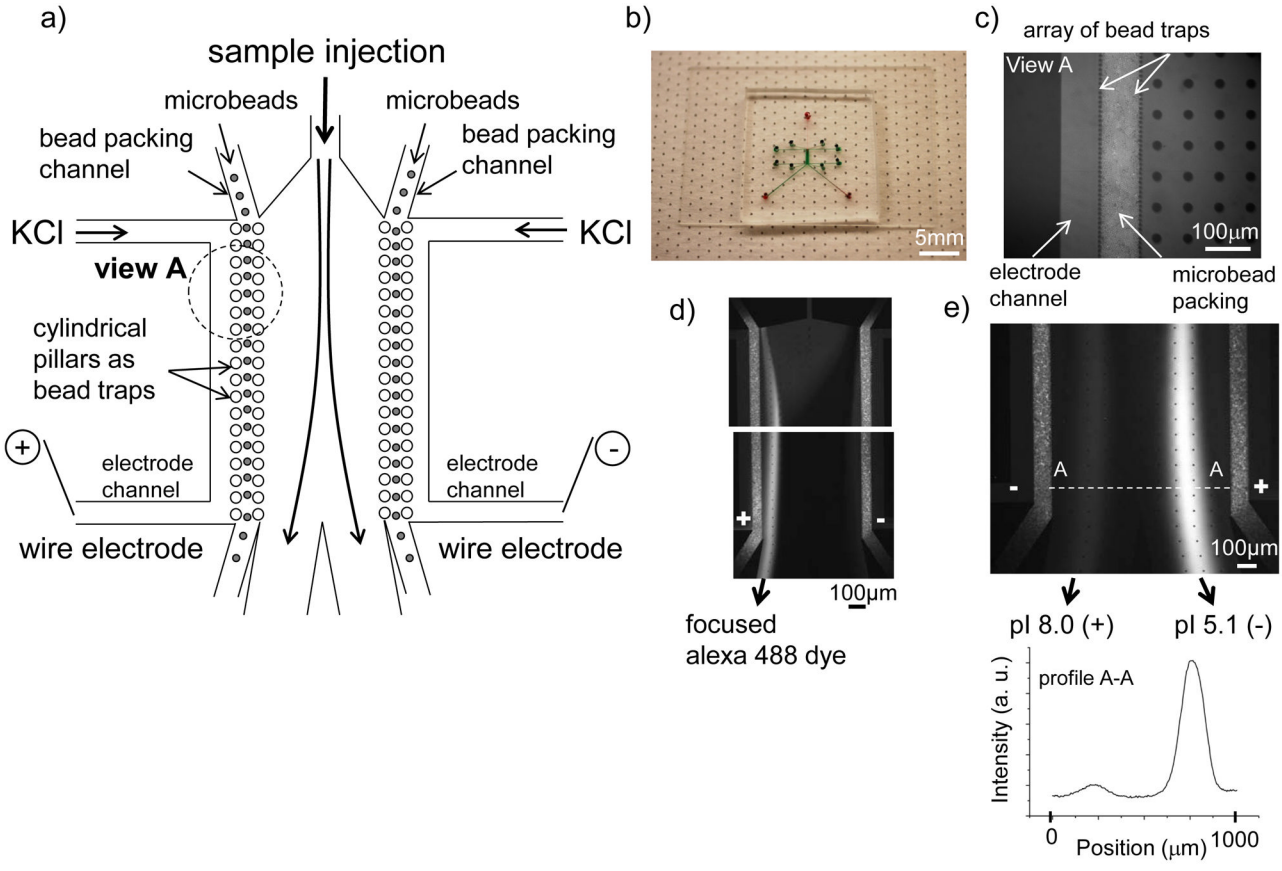

Figure 1.

Free-flow zone electrophoresis (FFZE) device for continuous-flow sorting of biomolecules. a) Schematic of the device. The electrical connection was created by inserting the Pt wires into the outlets of the electrode channels. b) A sorting device in PDMS with a micrograph of the device. c) Micrograph of a microbead membrane out of 6 μm polystyrene beads. d) Continuous-flow separation of fluorescent molecules, negatively charged Alexa Fluor 488 dye (1 μg/L), in pH 7.0 phosphate buffer solution at 5mM. The dye stream was deflected towards the anode. The applied field was $V_{applied}$ = 50 V across 1mm wide channel at a sample flow rate of 1 μL/min. The bead membrane consisted of 3μm silica beads. e) Using the same device with 3μm silica bead membranes, a mixture of two pI markers (pI 5.0 and 8.1) was separated into two different outlets at $V_{applied}$ = 50 V.

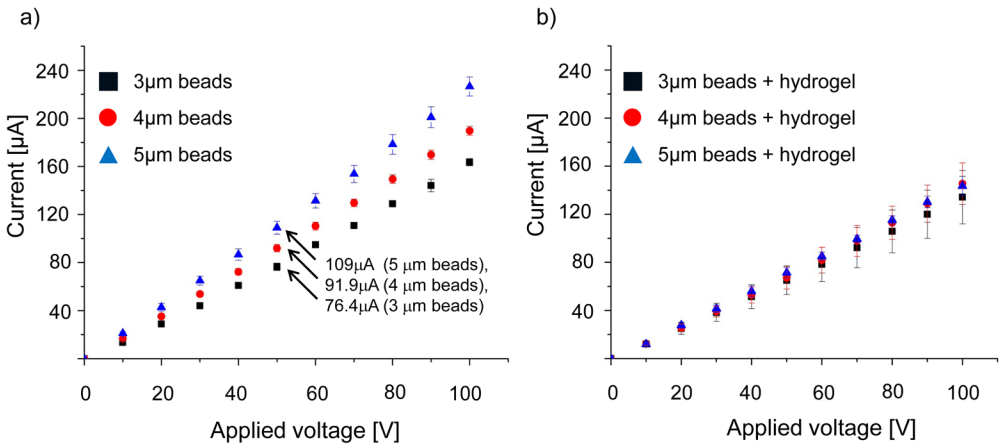

Figure 2.

Characterization of the microbead membranes with a measurement of I–V curves at different bead sizes (3, 4, 5 μm). a) The result shows a linear dependency of the total current from the applied voltage. Increasing bead size allowed higher total current coupling into the device due to larger pore size. b) I–V characterization of the microbead membranes infiltrated with a hydrogel. The total current was less dependent from the bead size because of the infiltrated hydrogel. At higher voltages above ~70 V, however, the difference between the bead sizes became noticeable.

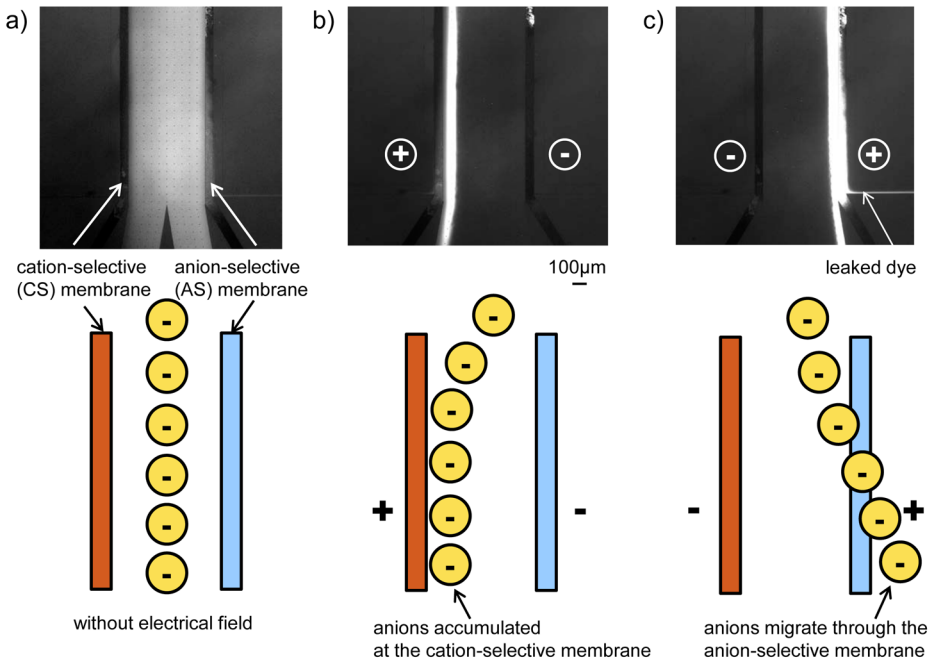

Figure 3.

Infiltration of a hydrogel solution to modify the surface charge of the microbead membrane (3 μm beads) for binary sorting. a) To minimize the sample loss through the nanoporous bead membranes, we have infiltrated cation- (CS) and anion-selective (AS) hydrogel into the microbead matrix on the anodic and cathodic side, respectively. A negatively charged dye inside the channel before applying electric field, b) the negatively charged dye cannot pass through the cation-selective membrane inside the sorting channel at 1μL/min and $V_{applied}$ = 120 V. c) After the polarity of the electrodes was reversed, the negatively charged AlexaFluor 488 dye could pass through the anion-selective membrane into the electrode reservoir. The leaked dye was migrating towards the anode.